Electronic Supplementary Information (SI) for:

The Chain Length Effect on Thermal Transport in Amorphous Polymers and A Structure-Thermal Conductivity Relation

Xingfei Wei*, [a] and Tengfei Luo*, [a, b, c]

[a]Department of Aerospace and Mechanical Engineering, [b]Department of Chemical and Biomolecular Engineering, [c]Center for Sustainable Energy at Notre Dame (ND Energy), University of Notre Dame, Notre Dame IN 46556, United States
*Corresponding authors: Xingfei Wei, xwei2@nd.edu, (574) 904-6870 and Tengfei Luo, tluo@nd.edu, (574) 631-9683.

1. Supplemental Simulation Models and Methods

A single PE chain from PE5 to PE200 is built by Moltemplate. [1] The Optimized Potential for Liquid Simulations of United Atom (OPLS-UA) force field is used to simulate the PE chains with the hydrogens lumped to the carbons. [2,3] All the molecular dynamics (MD) simulations in this study are carried by LAMMPS with a timestep of 1 fs. [4] The single chain PE with different chain lengths are relaxed under NPT (1 atm, 300 K) and NVT (300 K) ensembles until the chains are collapsed and the density of the small box is > 0.6 g/cm^3. To simulate a bulk amorphous polymer, the single chains of different lengths are duplicated to make the total size of the simulation box ~ $150 \times 150 \times 150$ Å^3. The total number of carbons is kept constant at 80000, and as a result we have 8000 chains for the PE5 simulation and 200 chains for the PE200 simulation. The bulk polymer models are relaxed at 600 K under many NPT (1 atm) and NVT ensembles iterations, until the density and radius of gyrations (R_g) are converged. To achieve the polymers in amorphous state at 300 K, the models are quenched from 600 K to 300 K under NPT (1 atm, 300 K) ensembles followed by NVT (300 K) ensemble optimizations. Before the productive NVE ensemble, a final simulation of 1 ns NPT (1 atm) and 0.5 ns NVT runs are performed, during which the density and R_g are also calculated. The thermal conductivities at different chain lengths are calculated at both 600 K and 300 K under NVE ensembles for 10 ns. Since PE5 is in gas state at 600 K, its thermal conductivity is not calculated at 600 K. Figure 1a in the main text shows the conformations of one single chain in the bulk models from PE5 to PE200 at 300 K. Since the models at 300 K are quenched from the 600 K models, the chain conformations for different chain lengths at 600 K are similar to those at 300 K.

The non-equilibrium MD (NEMD) simulation method is used to calculated the polymer thermal conductivity (Fig. 1 in main text). Using Langevin thermostats, a heat source of size 10 Å is set in the middle of the box, and two heat sinks of size 5 Å are set at the edges of the box. Due to the periodic boundary conditions, the two heat sinks are combined into one heat sink. The accumulative energy addition at the heat source and energy subtraction at the heat sink are recorded every 1000 steps (Fig. S1a). The temperature distribution across the polymer is calculated by averaging a block sized of 2 Å and over a time period of 4000 steps (Fig. S1b). At steady state, the heat flux is calculated by $J = \frac{dQ}{Adt}$, the temperature gradient is obtained by fitting $\frac{dT}{dx}$, the thermal

conductivity is calculated by Fourier's law $k = \frac{-J}{dT/dx}$. The total heat flux can also be calculated by summarizing energy convection and heat transfer through nonbonding (N_{pair}), bond stretching (N_{bond}), angle bending (N_{angle}) and dihedral torsion interactions ($N_{dihedral}$). [5-8]

$$J_x = \frac{1}{V}[\sum_i e_i v_{i,x} - \sum_i (S_i^{xx} v_{i,x} + S_i^{xy} v_{i,y} + S_i^{xz} v_{i,z}] \quad (1)$$

$$\begin{aligned} S_i^{ab} = -[& m_i v_{i,a} v_{i,b} + \frac{1}{2}\sum_{i,j=1}^{N_{pair}} (r_{i,a}F_{i,b} + r_{j,a}F_{j,b}) \\ & + \frac{1}{2}\sum_{i,j=1}^{N_{bond}} (r_{i,a}F_{i,b} + r_{j,a}F_{j,b}) \\ & + \frac{1}{3}\sum_{i,j,k=1}^{N_{angle}} (r_{i,a}F_{i,b} + r_{j,a}F_{j,b} + r_{k,a}F_{k,b}) \\ & + \frac{1}{4}\sum_{i,j,k,l=1}^{N_{dihedral}} (r_{i,a}F_{i,b} + r_{j,a}F_{j,b} + r_{k,a}F_{k,b} + r_{l,a}F_{l,b})] \end{aligned} \quad (2)$$

where J_x is the heat flux in the x-direction, V is the volume of the system, e_i is the total energy of particle i, $v_{i,x}$ is the x-component velocity of particle i, S_i^{ab} is the stress on particle i and a,b denote x, y or z in Cartesian coordinates, m_i is the mass, $r_{i,a}$ is the a-component position, $F_{i,b}$ is the b-component force. Since every particle has zero net charge, the nonbonding interaction only includes Lennard-Jones (LJ) interaction. The bonding interaction includes bond stretching, angle bending and dihedral torsion interactions.

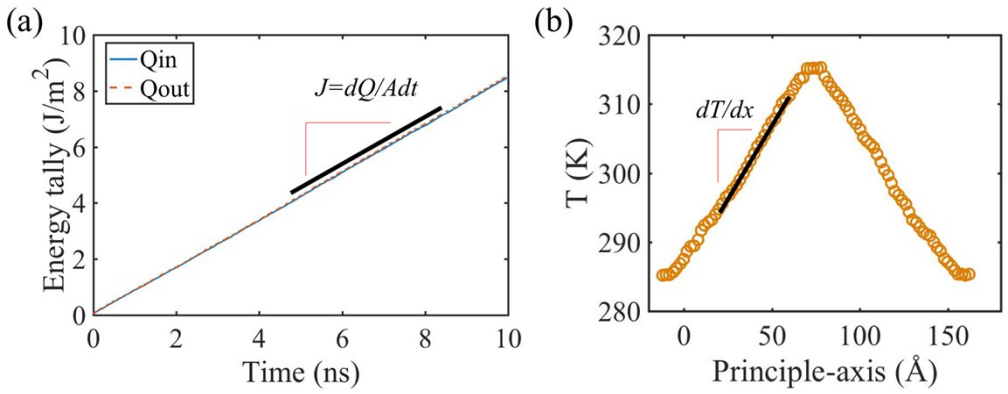

Figure S1. (a) The energy tally recorded at the thermostats. (b) The temperature distribution across the polymer at steady state.

2. Supplemental Results

Figure S2 shows the mass density and the number of bonds per atom change when the chain length increases from PE5 to PE200. Figure S3 shows the distribution of R_g at 300 K for PE with different chain lengths. Figure S4 shows direct relationships between (a) thermal conductivity and bond per particle, (b) thermal conductivity and number density, (c) thermal conductivity and R_g, (d) thermal conductivity and ξ.

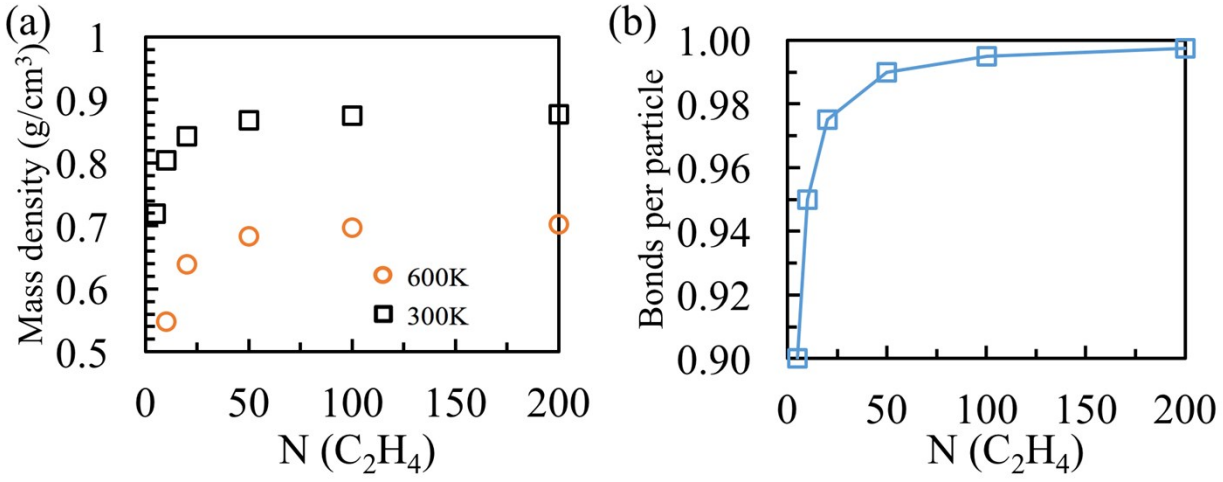

Figure S2. (a) The mass density and (b) the number of bonds per particle change with the chain length increasing from PE5 to PE200.

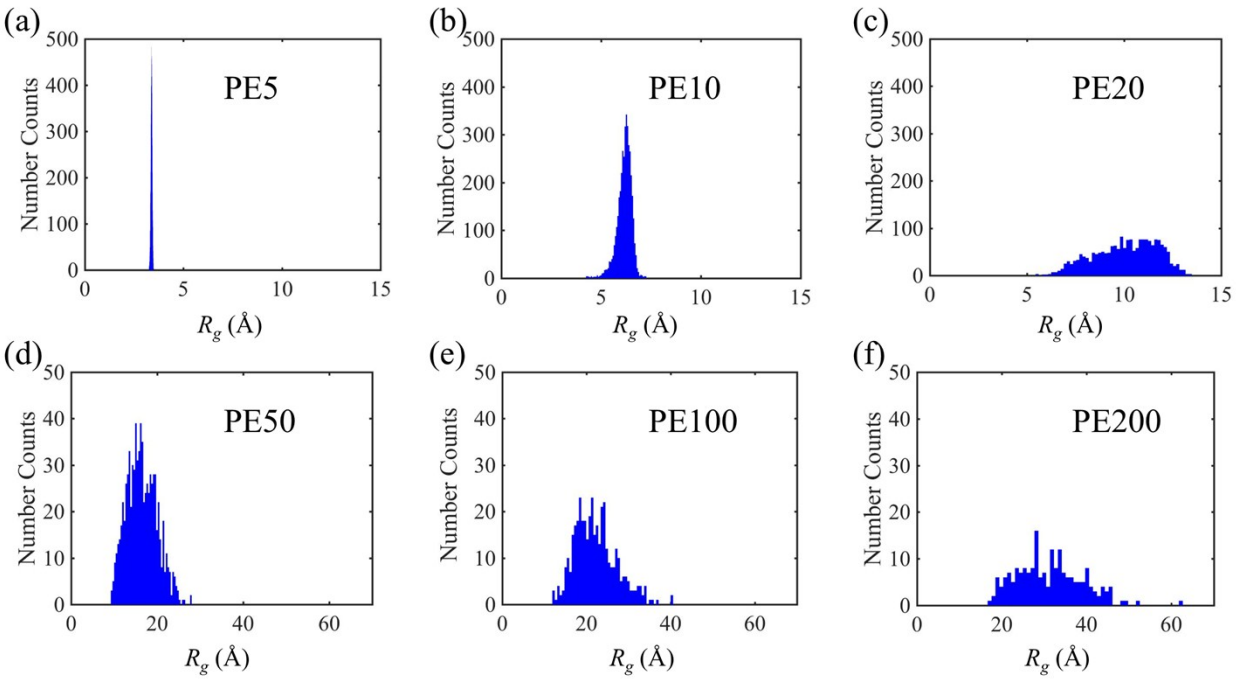

Figure S3. (a) - (e) The distribution of R_g for PE5 - PE200 with different chain lengths at 300 K.

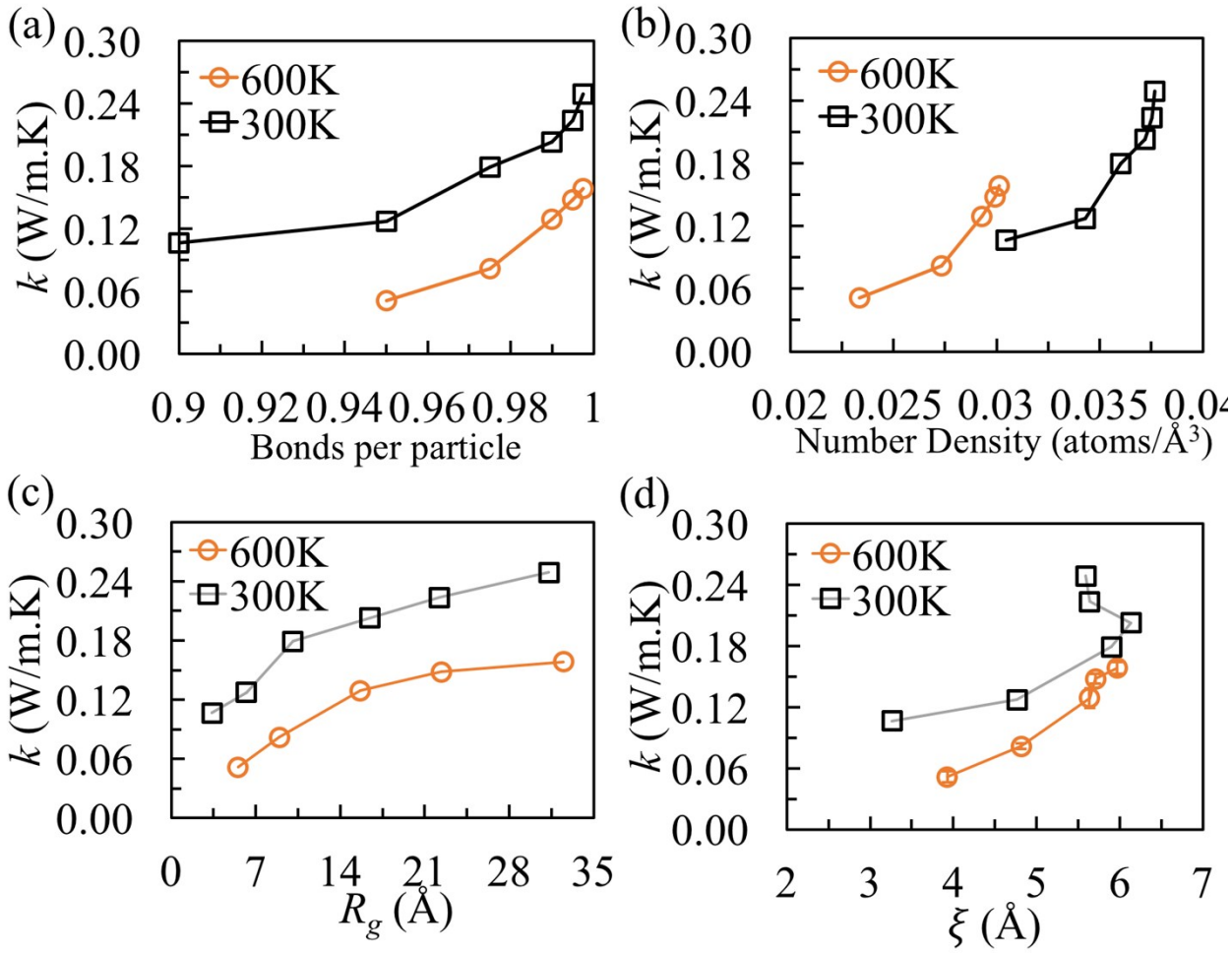

Figure S4. The relationship between PE thermal conductivity and (a) the number of bonds per particle, (b) the number density, (c) the chain conformation (R_g) and (d) the chain stiffness (ξ).

Figure S5 shows the heat flux calculated by Eq. (1) compared with the heat flux calculated from the thermostats. The heat flux calculated from the energy tally at the thermostats is used to calculated the polymer thermal conductivity. Although Eq. (1) underestimates the total heat flux, by normalizing the heat flux calculated by Eq. (1) into the heat flux calculated from the thermostats, the overall thermal conductivity can be decomposed into different contributions. Figures S6 and S7 shows the total heat flux decomposed into convection, nonbonding interaction, bond stretching, angle bending, and dihedral torsion interactions, for PE50 at 600 K (Fig. S6) and 300 K (Fig. S7). The bond stretching, angle bending, and dihedral torsion are summed as the bonding interaction contribution, which represent the heat transfer along the polymer chain. Figure S8 shows the percentagewise plot of thermal conductivity contributions (PE5 to PE200) at 600 K and 300 K.

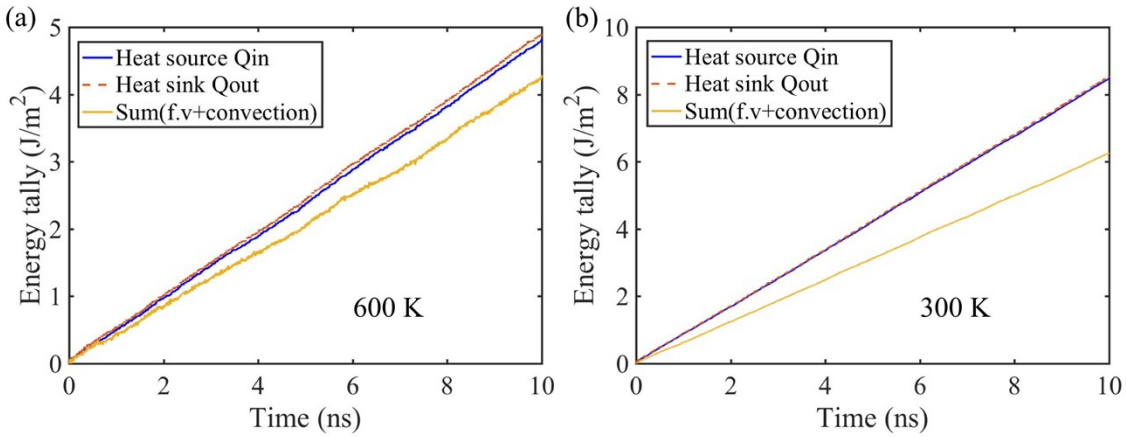

Figure S5. Using PE50 as an example to show the heat flux (the slope of the lines) calculated at (a) 600 K and (b) 300 K. The heat flux calculated from he energy tally on the two thermostats are compared to that calculated by summing the heat transfer through different force interactions and energy convection.

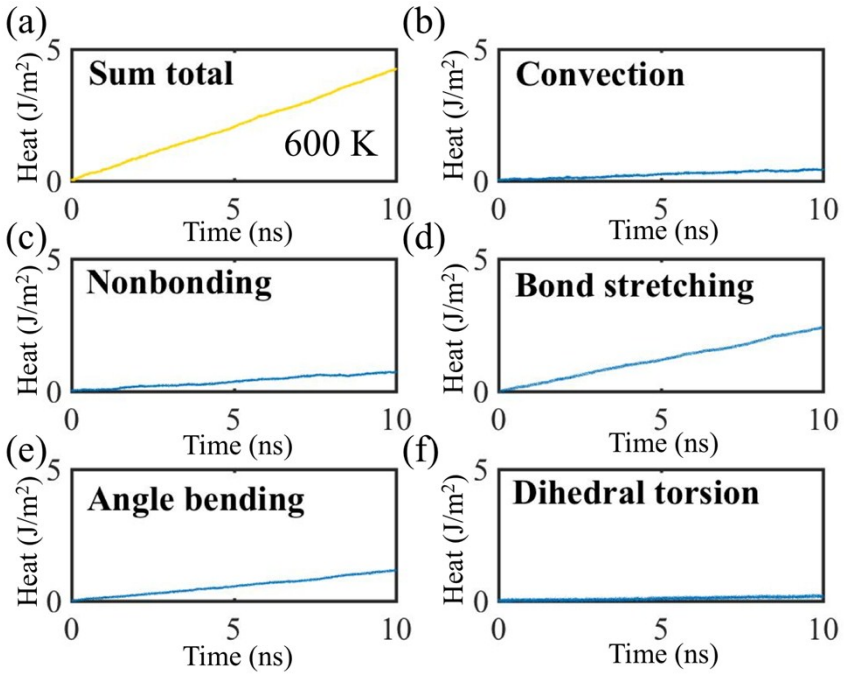

Figure S6. Using PE50 as an example to show (a) the total heat flux at 600 K decomposition into (b) energy convection, heat transfer through (c) nonbonding, (d) bond stretching, (e) angle bending and (f) dihedral torsion force interactions.

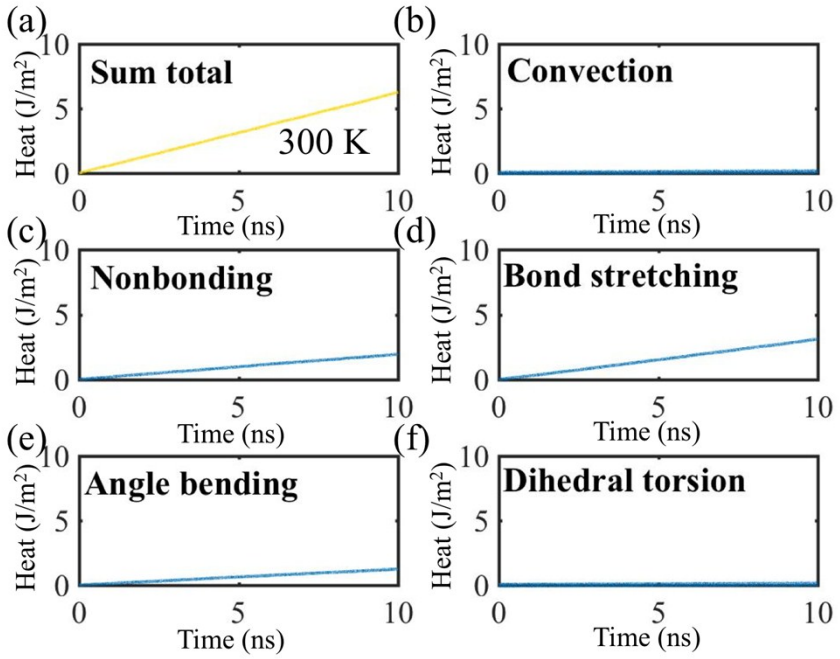

Figure S7. The same as Fig. S6 except that the heat flux is calculated at 300 K.

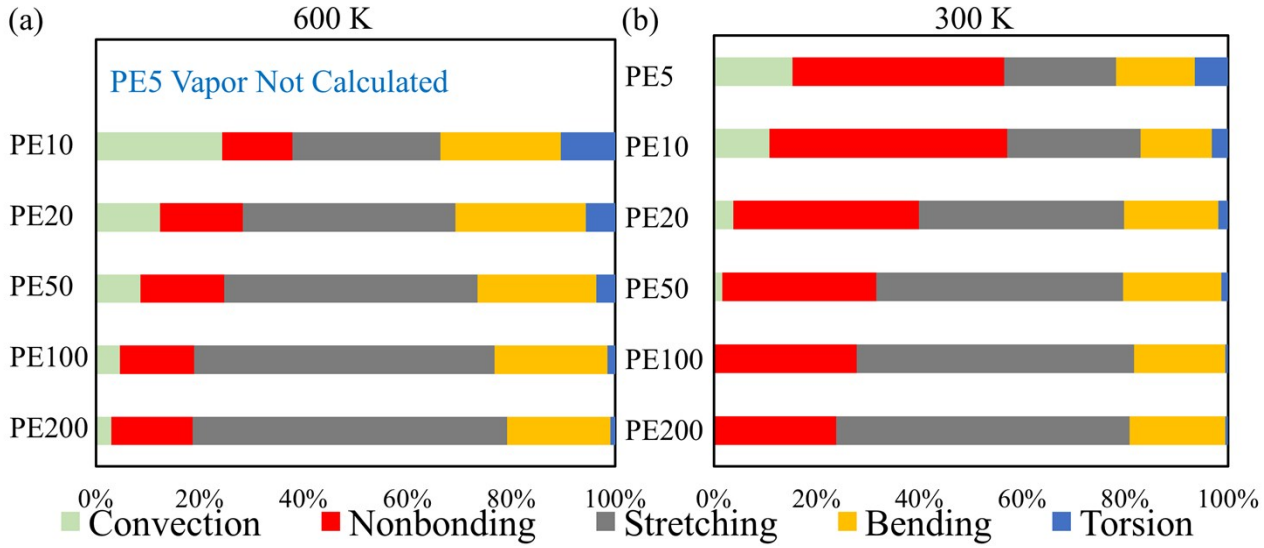

Figure S8. The heat flux decompositions into energy convection, and energy transfer through nonbonding, bond stretching, angle bending and dihedral torsion force interactions, at (a) 600 K and (b) 300 K for different chain lengths.

Figure S9 shows all 16 relationships between 4 different decomposed thermal conductivity values and four structural parameters. The four thermal conductivity values are k-total, k-convection, k-nonbonding and k-bonding, and k-total = k-convection + k-nonbonding + k-bonding. The four valuables are bonds per particle, n (number density), R_g and persistence length (ξ). The 4 selected relationships are marked with red boxes (Fig. S8), namely the relationships of k-convection and R_g, k-nonbonding and n, k-bonding and R_g, k-bonding and ξ.

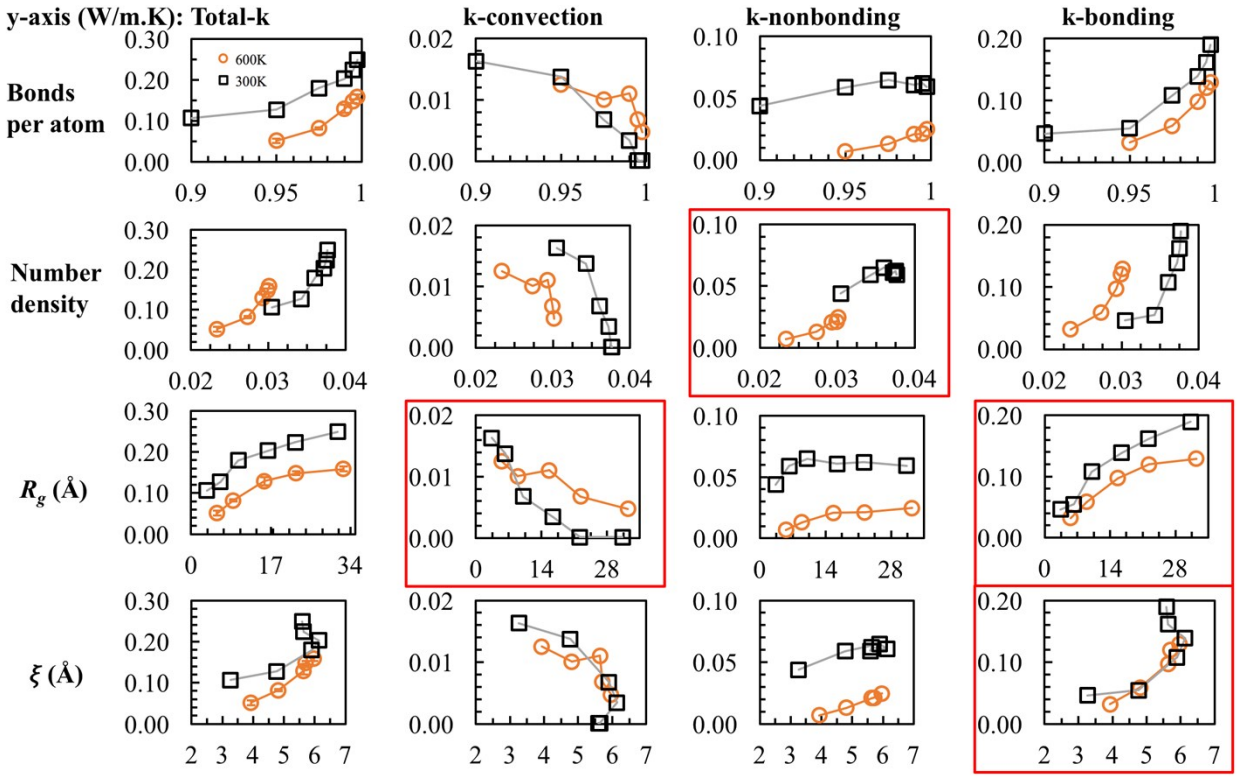

Figure S9. All the 16 relationships between total thermal conductivity (total-*k*), *k*-convection, *k*-nonbonding, *k*-bonding and number of bonds per particle, number density (n), R_g, ξ. The four selected relationships for modeling construction are outlined in red.

Table S1 shows the speed of sound in the longitude (V_l) and transverse (V_t) directions for PE with different chain lengths, the longitude speed of sound: $V_l = \sqrt{\frac{K + 4/3G}{\rho}}$, transverse speed of sound: $V_t = \sqrt{\frac{G}{\rho}}$, where K is the bulk modulus, G is the shear modulus and ρ is the mass density. When then chain length is larger than PE50, it turns out the speeds of sound converge to constant values.

Table S1. The speed of sound in the longitude (V_l) and transverse (Vt) directions.

	Chain length	ρ (g/cm^3)	Modulus (GPa)		Speed of sound (m/s)	
			Bulk	Shear	V_l	V_t
300 K	PE5	0.720	2.83	0.88	2357	1106
	PE10	0.804	5.75	1.29	3047	1264
	PE20	0.842	6.77	0.85	3062	1003
	PE50	0.868	6.67	1.53	3167	1327
	PE100	0.875	6.74	1.35	3126	1244
	PE200	0.878	6.65	1.40	3114	1262
600 K	PE10	0.548	2.49	0.39	1936	697
	PE20	0.639	3.73	1.15	2498	1166
	PE50	0.683	4.15	1.10	2544	1127
	PE100	0.697	4.35	1.32	2642	1226
	PE200	0.702	4.42	1.07	2581	1105

References

1 J. W. Ponder, TINKER: Software tools for molecular design. *Washington University School of Medicine, Saint Louis, MO,* 2004, **3**.

2 W. L. Jorgensen, D. S. Maxwell and J. Tirado-Rives, Development and testing of the OPLS all-atom force field on conformational energetics and properties of organic liquids. *J. Am. Chem. Soc.,* 1996, **118**, 11225-11236.

3 J. W. Ponder and F. M. Richards, An efficient newton-like method for molecular mechanics energy minimization of large molecules. *J. Comput. Chem.,* 1987, **8**, 1016-1024.

4 S. Plimpton, P. Crozier and A. Thompson, LAMMPS-large-scale atomic/molecular massively parallel simulator, http://lammps.sandia.gov. *Sandia National Laboratories,* 2007, **18**.

5 X. Wei, T. Zhang and T. Luo, Chain conformation-dependent thermal conductivity of amorphous polymer blends: the impact of inter-and intra-chain interactions. *Phys. Chem. Chem. Phys.,* 2016, **18**, 32146-32154.

6 X. Wei and T. Luo, The effect of the block ratio on the thermal conductivity of amorphous polyethylene–polypropylene (PE–PP) diblock copolymers. *Phys. Chem. Chem. Phys.,* 2018, **20(31)**, 20534-20539.

7 T. Ohara, T. Chia Yuan, D. Torii, G. Kikugawa and N. Kosugi, Heat conduction in chain polymer liquids: Molecular dynamics study on the contributions of inter-and intramolecular energy transfer. *J. Chem. Phys.,* 2011, **135**, 034507.

8 H. Matsubara, G. Kikugawa, T. Bessho, S. Yamashita and T. Ohara, Molecular dynamics study on the role of hydroxyl groups in heat conduction in liquid alcohols. *Int. J. Heat Mass Transfer,* 2017, **108**, 749-759.